Crack Shear-Slip in Reinforced Concrete Elements

Frank J. Vecchio[1] and Derek Lai[2]

Received 17 November 2003, accepted 19 March 2004

Abstract

A calculation procedure is described for estimating crack shear stresses and crack slip displacements from average strain measurements made on reinforced concrete panels. Several series of panels, previously tested, are examined and crack shear-slip data are extracted. These data are compared against the predictions of previously developed crack slip models, as well as against an alternative constitutive model proposed herein. Reasonable correlation is found between experimental and calculated values, particularly at near-ultimate load conditions. It is then shown that including crack shear slip behaviour in a computational model results in improved accuracy in terms of predicted load-deformation response and ultimate load capacity for reinforced concrete elements such as panels, beams and shear walls. Further, it is shown that rigorously accounting for crack slip displacements results in a better representation of various subtle aspects of behaviour, such as the failure mode and the capacity of elements to deform and redistribute load.

1. Introduction

In the development of nonlinear finite element procedures for modelling the behaviour of reinforced concrete elements subjected to general in-plane stress conditions, formulations have generally proceeded in one of two directions; either where cracks are considered to be smeared within the concrete continuum or where cracks are considered to be discrete and accounted for in the meshing of the structure. In the context of smeared crack models, a further subdivision occurs depending on whether the crack orientations are taken as fixed or allowed to rotate. With rotating-crack models, it is assumed that a gradual reorientation occurs in the crack direction, as dictated by the loading or material response. Along with the change in crack direction, a gradual reorientation is assumed to occur in the principal stress and strain directions in the concrete. Conversely, with fixed-crack models, the crack direction remains fixed in the direction of first cracking; in some formulations, if stress conditions dictate, new cracks may form at alternate inclinations. An important aspect of the fixed-crack approach is that shear stresses may develop on the crack surfaces and crack shear slip may occur as a result. Rotating crack models, in general, do not account for crack shear slips in the formulation of the element constitutive response.

The Modified Compression Field Theory (MCFT), developed by Vecchio and Collins (1986), is one possible model shown to provide reasonably consistent and accurate simulations of reinforced concrete behaviour. It is, in essence, a rotating smeared-crack model that represents concrete as an orthotropic material wherein equilibrium, compatibility, and constitutive relations are formulated in terms of average stresses and average strains. Also central to the model, however, is the consideration of local stress conditions at crack locations. Local shear stresses on crack surfaces are calculated and checked against a limiting value. If the crack shear stresses become excessive, reductions are made to the post-cracking tensile stresses in the concrete. However, crack shear slips associated with the shear stresses are not explicitly calculated nor accounted for in the element deformations.

The Disturbed Stress Field Model (DSFM) was proposed by Vecchio (2000, 2001) as an alternative formulation. Relative to the MCFT, the DSFM attempts to provide a better phenomenological representation of the behaviour of concrete by explicitly allowing for crack shear slip in the description of element deformation. It dispenses with the condition that average principal stress and average principal strain directions remain coincident, and removes the crack shear stress check that was found to be troublesome and sometimes ignored by others in their interpretation or implementation of the MCFT. In relating crack shear slips to crack shear stresses, the DSFM incorporates a tentative formulation based on the work of Walraven and Reinhardt (1981) in recognition of its relative simplicity and proven accuracy.

The mechanisms of crack shear transfer, also known as aggregate interlock action, have been studied extensively. In addition to Walraven (1981) and Walraven and Reinhardt, notable work has been done by Bazant and Gambarova (1980), Dei Poli et al. (1987), Okamura and Maekawa (1991), and Dei Poli et al. (1990), among others. The Walraven-Reinhardt fundamental model

[1]Professor, Dept. of Civil Engineering, University of Toronto, Toronto, Canada.
E-mail: fjv@civ.utoronto.ca
[2]Graduate Student, Dept. of Civil Engineering, University of Toronto, Toronto, Canada.

was based on a statistical analysis of the crack structure and associated contact areas between crack faces; crack shear stresses were formulated as functions of crack normal and tangential displacements. The rough crack model proposed by Bazant and Gambarova expanded on the previous work, developing formulations for constitutive response better suited for nonlinear incremental analyses. It is important to note that the data used to develop and calibrate these crack slip models were largely derived from 'push-off' or 'pull-off' specimens of the type shown in **Fig. 1(a)**.

In work leading to the formulation of the MCFT, and in subsequent experimental investigations, a large number of reinforced concrete panels were tested using specially developed apparatus (see **Fig. 2**). A schematic representation of a typical panel element is shown in **Fig. 1(b)**. While data from these panels have been extensively studied with regards to determining the constitutive response of cracked concrete in compression and in tension, little attention was given to extracting information on crack shear behaviour.

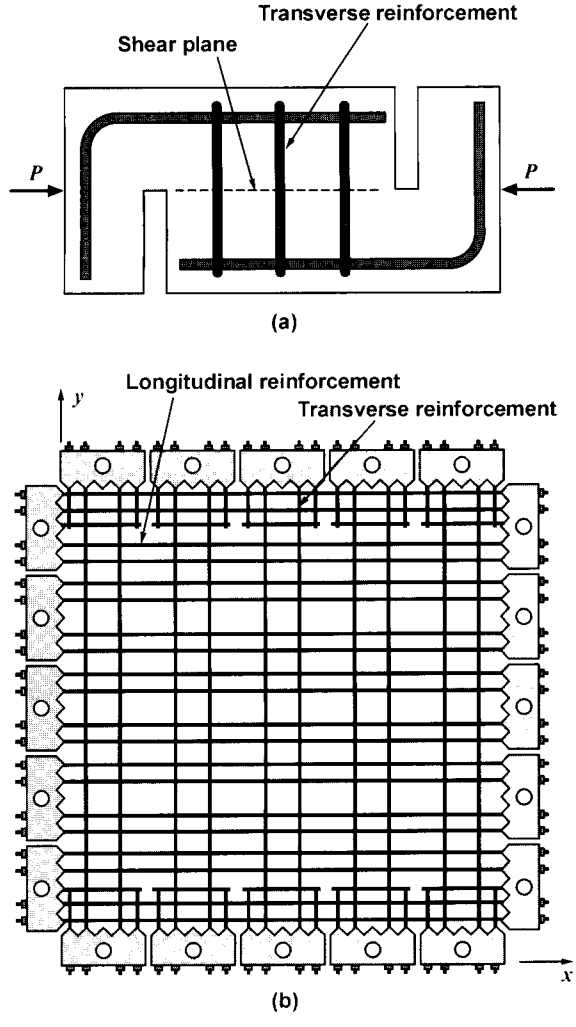

Fig. 1 Specimen types for studying crack shear slip
(a) Push-off specimen (b) Shear panel.

This paper re-examines a large body of test panel data with the aim of acknowledging and better understanding the nature and influence of crack shear behaviour inherent in the panels' response. The data are next compared against behaviour predicted by the models proposed by various researchers. The suitability of these models for implementation into the DSFM, or other conceptually similar fix- or rotating-crack models, is then assessed. The primary contributions of this paper are: (i) documentation of a calculation procedure for extracting crack shear stress-slip response from test panel data; (ii) demonstration that currently available models for crack shear slip correlate reasonably well with the data extracted from a large set of test panels; (iii) proposal of an alternate model combining the favourable features of two existing models; and (iv) discussion as to why it is important to consider crack shear-slip.

2. Crack shear-slip models

While a number of models are available for representing crack-shear (aggregate interlock) mechanisms, the most suitable for implementation into the Disturbed Stress Field Model are those by Walraven and Reinhardt (1981) and by Okamura and Maekawa (1991) owing to their simplicity and adaptibility to a secant stiffness-based formulation.

2.1 Walraven model:

An adaptation of the formulations proposed by Walraven and Reinhardt produces the following:

$$\delta_s = \frac{v_{ci} + v_{co}}{1.8w^{-0.8} + (0.234w^{-0.707} - 0.20) \cdot f_{cc}} \quad (1)$$

where δ_s is the tangential slip along the crack (mm), v_{ci} is the shear stress on the crack surface (MPa), w is the width of the crack (mm), and f_{cc} is the concrete cube strength (MPa). An initial offset in the crack shear-slip relation is provided by the term v_{co}, taken as follows:

$$v_{co} = \frac{f_{cc}}{30}. \quad (2)$$

Note that in this adaptation, the influence of local normal compressive stresses on the crack surfaces are not explicitly considered, but are nevertheless a factor in that they influence the crack width.

2.2 Okamura-Maekawa model:

The formulation proposed and utilized by Okamura and Maekawa in their fixed non-orthogonal crack model is given by:

$$\delta_s = w\sqrt{\frac{\Psi}{1-\Psi}} \tag{3}$$

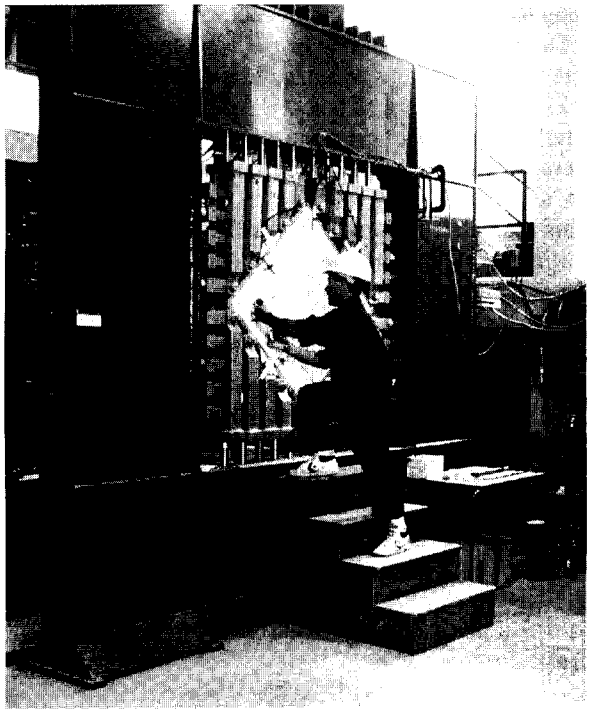

(a)

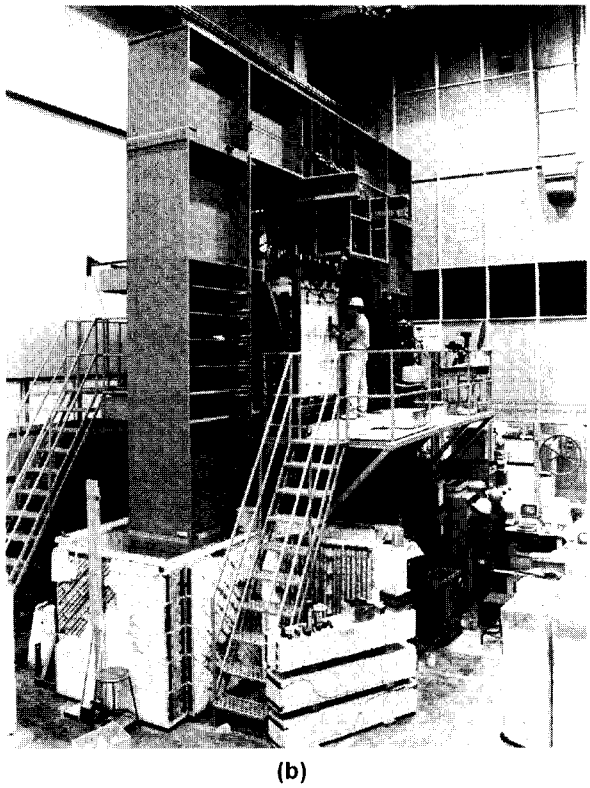

(b)

Fig. 2 Facilities used for panel tests (a) Panel Element Tester (b) Shell Element Tester.

where $$\Psi = \frac{v_{ci}}{v_{cmax}} \tag{4}$$

The term v_{cmax} represents the theoretical maximum shear stress that can be resisted on the crack, and was previously given by Vecchio and Collins (1986) as:

$$v_{cmax} = \frac{\sqrt{f'_c}}{0.31 + \frac{24\,w}{a+16}} \text{ (MPa).} \tag{5}$$

where a is the maximum aggregate size (mm) and f'_c is the concrete 28-day cylinder strength. The average crack width, w, can be estimated from the current principal tensile strain in the concrete, ε_1, and from the average crack spacing, s, as:

$$w = \varepsilon_1 \cdot s \tag{6}$$

Note that as v_{ci} approaches v_{cmax}, a shear slip failure occurs (i.e., δ_s becomes infinitely large).

2.3 Lai-Vecchio model:

The Walraven-Reinhardt formulation model introduces some instability into the computational algorithm because of the initial slip, represented by the v_{co} term. [That is, with a nonzero v_{co} term and little or no shear stress acting on the crack, slip can occur in either direction without discretion.] The Okamura-Maekawa formulation avoids this difficulty, and further provides the opportunity to better define the maximum shear stress that can be permitted on the crack; however, it was found to underestimate slip displacements at intermediate stress values. A combination of the two models, proposed here, attempts to avoid the limitations of each. Hence, it is proposed that:

$$\delta_s = \delta_2\sqrt{\frac{\Psi}{1-\Psi}} \tag{7}$$

where $$\delta_2 = \frac{0.5\,v_{cmax} + v_{co}}{1.8\,w^{-0.8} + (0.234\,w^{-0.707} - 0.20)\cdot f_{cc}} \tag{8}$$

and where Ψ and v_{cmax} are as previously defined. This formulation affords the opportunity to consider factors such as aggregate size in defining v_{cmax} (found to be important in high strength concrete), and remains consistent with previous formulations used with the MCFT.

The three constitutive models are compared in **Fig. 3** for two representative concrete strengths and three crack width conditions. (A maximum aggregate size of 20 mm was assumed in the calculations.) Note that while initial slip values vary, the stiffnesses of the responses are fairly consistent amongst the three models.

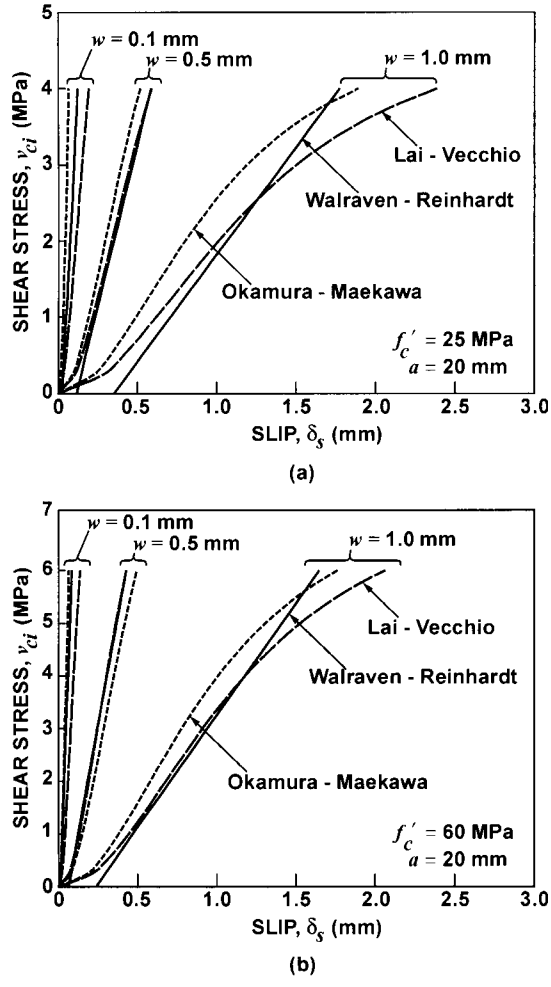

Fig. 3 Comparison of crack shear stress-slip models (a) For 25 MPa concrete (b) For 60 MPa concrete.

3. Procedure for calculating crack shear stresses and slips from panel test data

A reinforced concrete element, subjected to general stress conditions, may experience cracking. If so, local shear stresses may develop on the crack interfaces, depending on the loading and reinforcement conditions. The local shear stresses will ordinarily be accompanied by shear slip along the crack interfaces. The objective here is to relate the local shear stresses to the shear slips occurring on the crack surfaces, as manifested in test panels.

In the approach adopted, the deformation of a reinforced concrete element is considered to be composed of both continuum straining and discontinuous slip along crack surfaces, as shown in **Fig. 4**. The continuum straining is the result of mechanical compliance to stress and the smearing of crack widths over a finite area. The slip component is the result of rigid body movement along the crack interfaces. Relative to a reference x,y-system, strains measured on the surface of the element, over gauge lengths sufficiently long to span several cracks, will intrinsically contain both components of deformation. These measured (total) or 'apparent' strains will be denoted as $[\varepsilon] = \{\varepsilon_x\ \varepsilon_y\ \gamma_{xy}\}^T$. The inclination of the principal total strains, θ_ε, can be calculated using usual transformation procedures.

The actual (net) strains in the continuum will be denoted as $[\varepsilon_c] = \{\varepsilon_{cx}\ \varepsilon_{cy}\ \gamma_{cxy}\}^T$. It is these strains, shown in **Fig. 4(a)** that are to be employed in appropriate constitutive relations to determine average stresses from the average strains in the concrete. The actual inclination of the average principal strains in the continuum, θ, is again calculated from standard transformations. This inclination is assumed to equal the inclination of the average principal stresses in the concrete (θ_σ), and also defines the perpendicular crack direction.

Consider next the discrete slip occurring along the crack surfaces (**Fig. 4(b)**). Assume that the cracks are inclined in the direction of the concrete average principal tensile stress, that the cracks have an average width and spacing of w and s, respectively, and that the slip

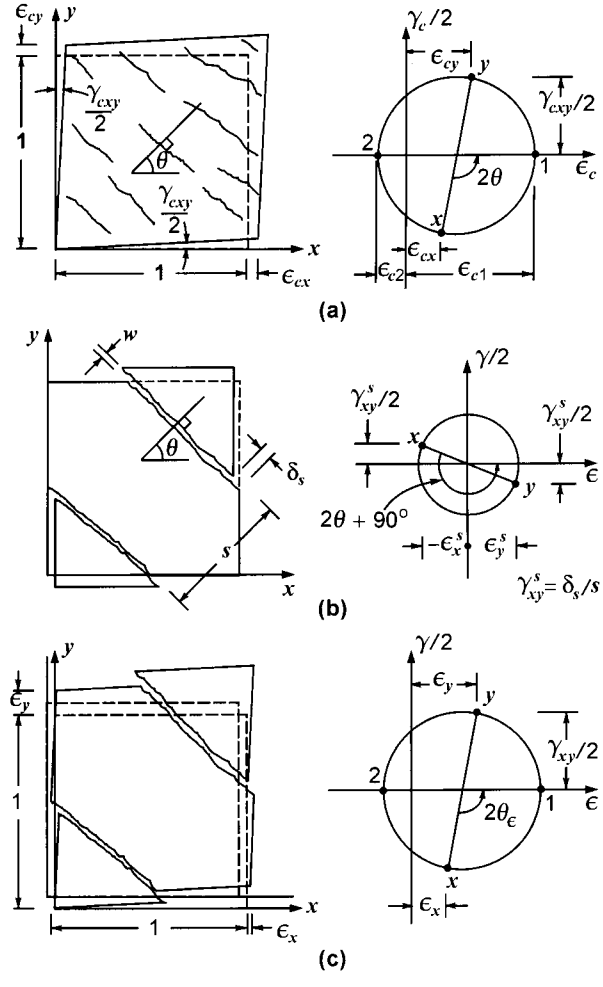

Fig. 4 Deformations of Panel Element (a) Due to average (smeared) continuum response (b) Due to slip along crack surfaces (c) Combined.

along the crack surface is of magnitude δ_s. One can define an average shear-slip strain as follows:

$$\gamma_s = \frac{\delta_s}{s} \tag{9}$$

Given the element total strains [ε], and the inclination of the net principal strains and stresses, θ_σ, one can calculate the average shear-slip strain from the following relationship:

$$\gamma_s = \gamma_{xy} \cdot \cos 2\theta_\sigma + (\varepsilon_y - \varepsilon_x) \cdot \sin 2\theta_\sigma \tag{10}$$

Assume that the reinforced concrete element is orthogonally reinforced, with the reinforcement ratios in the x- and y-directions given by ρ_x and ρ_y, respectively. Further, assume that the element is subjected to uniform stresses, $[\sigma] = \{\sigma_x \ \sigma_y \ \tau_{xy}\}^T$, applied along the element boundaries (see **Fig. 5(a)**). As a result, the element undergoes deformation, and the total strain condition is measured as [ε] as previously discussed.

From the measured strains in the x- and y-directions, the average strains in the reinforcement (f_{sx} and f_{sy}) can be calculated from an appropriate constitutive model. Given the reinforcement stresses and the applied load conditions, the average stresses in the concrete are then calculated as follows:

$$f_{cx} = \sigma_x - \rho_x \cdot f_{sx} \tag{11}$$

$$f_{cy} = \sigma_y - \rho_y \cdot f_{sy} \tag{12}$$

$$v_{cxy} = \tau_{xy} \tag{13}$$

Next, from standard transformations, the concrete principal stresses (f_{c1} and f_{c2}) and inclination of the average stress field, θ_σ, are found (see **Fig. 5(b)**). The value of θ_σ thus determined is used in Equation 10.

At a crack, it is assumed that the local principal tensile stress in the concrete diminishes to zero. Hence, in order for the average stress f_{c1} to be transmitted across the crack, there must be an increase in the local stresses in the reinforcement produced by an increment in the average principal tensile strain, $\Delta\varepsilon_{1cr}$. The local strains in the reinforcement will thus be

$$\varepsilon_{scrx} = \varepsilon_{sx} + \Delta\varepsilon_{1cr} \cdot \cos^2\theta_\sigma \tag{14}$$

$$\varepsilon_{scry} = \varepsilon_{sy} + \Delta\varepsilon_{1cr} \cdot \sin^2\theta_\sigma \tag{15}$$

and the local stresses, f_{scrx} and f_{scry}, can be calculated according to appropriate constitutive relationships. The value of $\Delta\varepsilon_{1cr}$ is found by satisfying the following equilibrium condition:

$$f_{c1} = \rho_x \cdot (f_{scrx} - f_{sx}) \cdot \cos^2\theta_\sigma + \rho_y \cdot (f_{scry} - f_{sy}) \cdot \sin^2\theta_\sigma \tag{16}$$

Once the local reinforcement stresses are known, then the local shear stress on the crack can be determined as follows:

$$v_{ci} = \rho_x \cdot (f_{scrx} - f_{sx}) \cdot \cos\theta_\sigma \sin\theta_\sigma - \rho_y \cdot (f_{scry} - f_{sy}) \cdot \sin\theta_\sigma \cos\theta_\sigma \tag{17}$$

Note that the formulations above are limited to orthogonally reinforced elements, and that elastic and plastic offset strains are not considered. A more comprehensive discussion, one that includes offset strains (e.g., Poisson's effects) and multiple non-orthogonal reinforcement, is given by Vecchio (2000). Also note that full bond and no dowel action have been assumed.

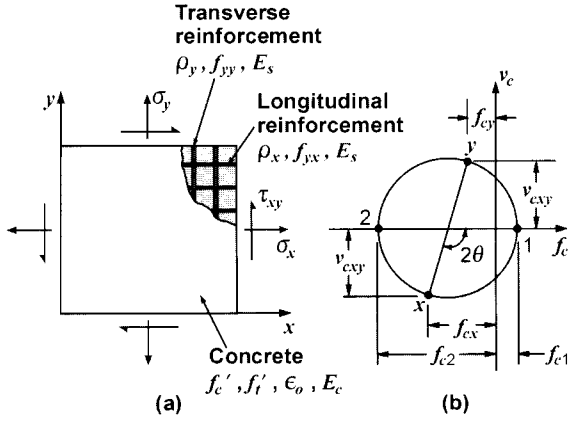

Fig. 5 Stress conditions in panel element (a) Loading and reinforcement conditions (b) Mohr's circle for average stresses in concrete.

4. Shear-slip data from test panels

The Panel Element Tester, developed in 1978, enabled the testing of 890 x 890 x 70 mm reinforced concrete panel elements under general conditions of in-plane stress (see **Fig. 2(a)**). In 1984, The Shell Element Tester was added, with the capability of loading 1525 x 1525 x 315 mm panels under various combinations of in-plane and out-of-plane stresses (see **Fig. 2(b)**). Since then, over 200 panels have been tested covering a wide range of structural parameters and loading conditions.

Selected for this study were only those panels subjected to monotonically increasing in-plane stresses. The PV-Series of panels, tested by Vecchio and Collins (1982), were generally orthogonally reinforced, constructed of normal strength concrete, and subjected to shear-dominant conditions. The PB-Series of panels, tested by Bhide and Collins (1989), were generally uniaxially reinforced, constructed of normal strength concrete, and tested under various combinations of uniaxial tension and in-plane shear. The PA- and PHS-Series panels, tested by Vecchio et al. (1994), were orthogonally reinforced, constructed of high strength concrete, and subjected to various combinations of biaxial

normal stresses and shear. In addition, the SE-Series of large-scale panels tested by Kirschner and Collins (1986) were considered. The Kirschner panels were tested using the Shell Element Tester; all others were performed on the Panel Element Tester.

For each test panel, at various stages through the course of testing, deformations were held constant while surface strain readings were taken, cracks were measured, and various other electronic instrumentation was scanned. [Readings took approximately 15 minutes to complete.] Hence, at each load stage, an accurate measure is known of the applied stress conditions (σ_x, σ_y, τ_{xy}) and of the resulting average total strains (ε_x, ε_y, γ_{xy}). Although there were visible signs of slip along the crack surfaces (for example, ridging and crushing of the concrete along the interfaces, and relative displacements of opposing faces), no attempt was made to monitor crack shear slips at that time. However, using the calculation procedure outlined above, the crack slips can be estimated. Assumptions are required regarding the average crack spacing, and the constitutive response of the embedded reinforcement. Precise test records were not maintained with regards to average crack spacings, although notes and photographic evidence suggest that the average spacing was in the range of 40 to 60 mm at intermediate and advanced stages of loading in the typical panel (generally, the more heavily reinforced panels had a smaller crack spacing). An average spacing of 50 mm is assumed here (200 mm for the larger SE panels). All reinforcement used in the construction of the panels was heat-treated; test coupons exhibited a highly ductile response with a well defined yield stress. Hence, the constitutive response assumed for the reinforcement, for both the average and local behaviour, is bilinear (elastic-plastic). [Also note that the reinforcement was typically small diameter deformed wire or welded wire mesh; as such, dowel action and bond slip were negligible factors.] Calculations were made of the shear stress on the crack, and the resulting crack shear slip, for each panel at each load stage. See Appendix I for a sample calculation.

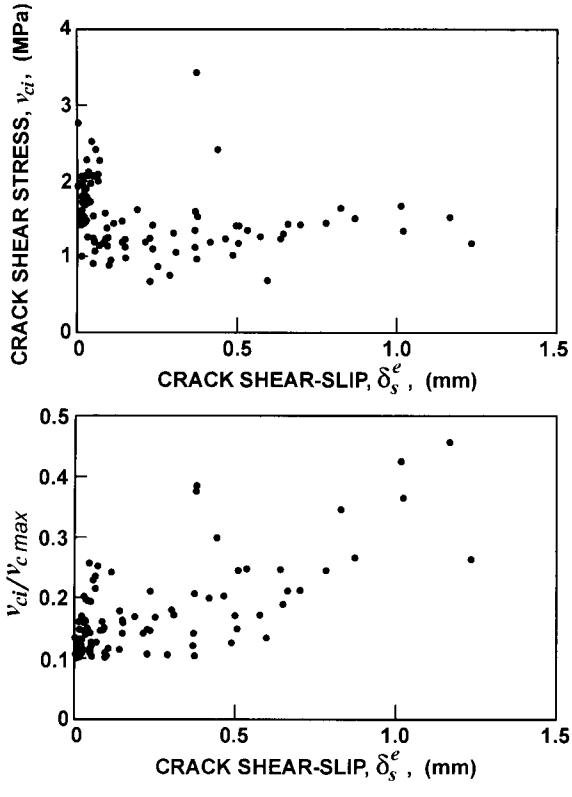

Fig. 6 Crack shear slips from test panels (a) Variation with crack shear stresses (b) Variation with normalized crack shear stress.

Shown in **Fig. 6** is the resulting crack shear stress-slip response determined for all panels considered. As one might expect, the results are widely scattered; in part due to the assumptions in the calculation procedure, and in part due to the intrinsic nature of the mechanisms involved. To reduce the scatter somewhat, only points where $v_{ci}/v_{cmax} > 0.1$ are considered.

5. Correlation of panel data to crack-slip models

Shown in **Fig. 7** are comparisons of the experimental crack shear slips against those computed using each of the three models previously described: Walraven-Reinhardt, Okamura-Maekawa, and Lai-Vecchio. Again, there is considerable scatter, particularly for points corresponding to early loading stages where the average crack spacings were in a transitional stage and had not yet approached the final (assumed) value. At early load stages, the typically larger than assumed crack spacings resulted in wider than calculated crack widths, and hence larger than calculated crack shear slips.

Figure 8 provides an indication of the correlation provided by the analytical models when plotted against increasing shear stress. In general, as the stresses increase, the ratio of the observed to predicted crack slip achieves a tighter correlation. None of the three models shows remarkably better correlation than the others. All three appear to provide a reasonably accurate portrayal of the crack shear-slip phenomenon, particularly at advanced stages of loading where the slip mechanism assumes greater importance in influencing the behaviour of an element.

It is worth noting, at this point, that the correlations achieved promote confidence in the analytical procedures despite the high scatter. Bearing in mind that the Walraven-Reinhardt model was developed based on data derived from significantly different test conditions, and that the Okamura-Maekawa model was based on a substantially different analysis philosophy, the correlations are surprisingly good. This general compliance

was by no means assured a priori, given the number of assumptions made in the formulation of the DSFM and in the method used to analyse the test data. That the Walraven-Reinhardt model, in particular, should provide such reasonable correlations gives strength to the DSFM approach to incorporating crack shear slips into a rotating crack model. More specifically, it indicates that the DSFM method of accounting for post-cracking tensile stresses in the concrete, and the method of calculation of stresses in the reinforcement, leads to the calculation of shear stresses and shear slips on the crack surfaces that are consistent with widely accepted aggregate interlock models.

It is fair to say that the proposed Lai-Vecchio formulation offers no real improvement in correlations to the

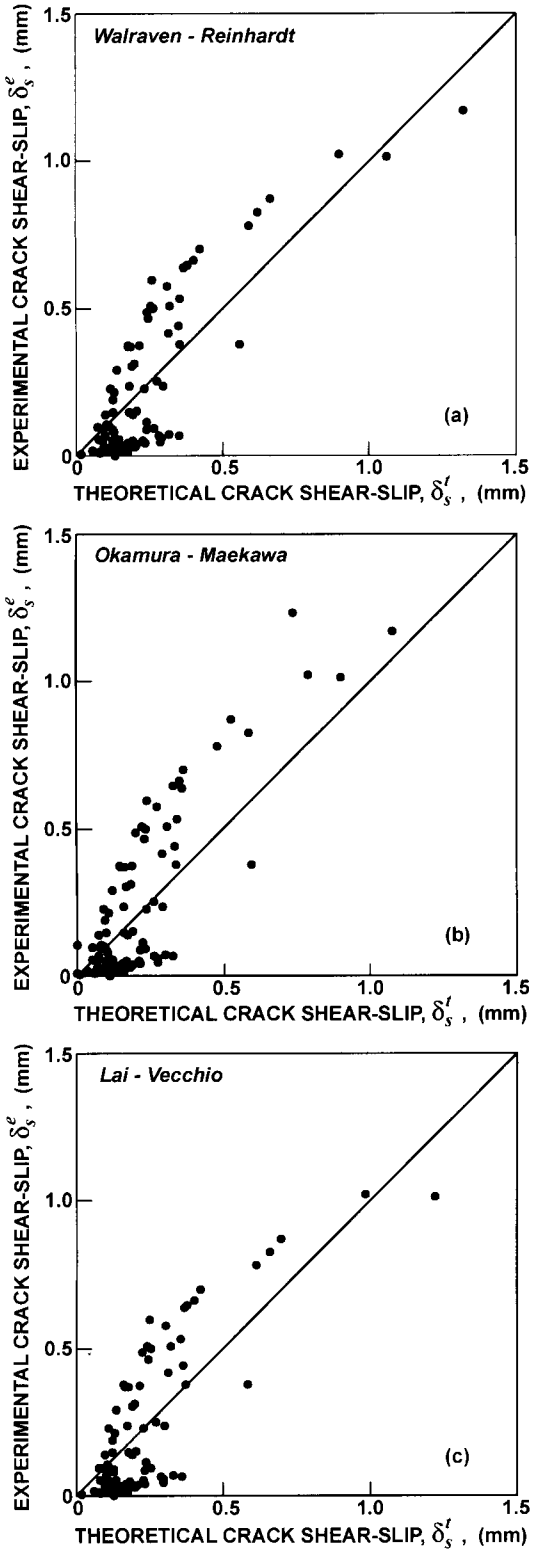

Fig. 7 Comparison of experimental and theoretical crack shear slips (a) Walraven-Reinhardt model (b) Okamura-Maekawa model (c) Lai-Vecchio model.

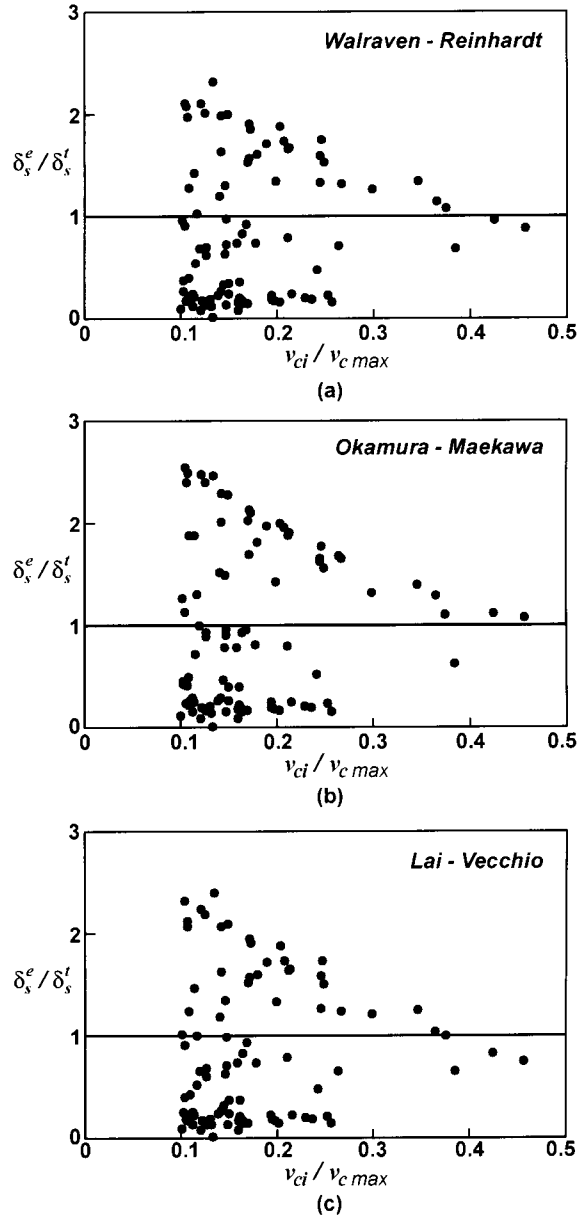

Fig. 8 Correlation of predicted crack shear slips (a) Walraven-Reinhardt model (b) Okamura-Maekawa model (c) Lai-Vecchio model.

test data relative to the other two models. Its value is derived from an ability to accept improved expressions for v_{cmax}, as they become available, and from better numerical stability and ease of implementation. It will also allow for the consideration of different aggregate types, such as expanded shale or crushed stone, and fibre reinforcement.

6. Implementation in finite element analyses

The various crack shear slip models discussed were incorporated into a nonlinear finite element algorithm. Details of the finite element procedure are provided by Vecchio (2001).

To gauge the value of including crack slip modelling in the analysis of reinforced concrete structural elements, and to assess the relative accuracy of the formulations available, nonlinear finite element analysis studies were then undertaken. Several series of panels, beams and shear walls were examined; for each, analyses were undertaken with and without crack shear slips considered. When considered, crack shear slips were alternately modelled using the Walraven-Reinhardt, Okamura-Maekawa and Lai-Vecchio models in the context of the Disturbed Stress Field Model. When crack shear slip was not considered, the analyses were done in the context of the Modified Compression Field Theory. All other constitutive models and structural modelling parameters were maintained identical across the four sets of analyses for each specimen examined.

The panel elements considered included the PV-, PB-, PA/PHS-, and SE-Series as previously described. All panels were modelled using a single-element mesh and a load-increment approach. Comparisons of the experimental and computed ultimate shear capacities of the panels are given in **Table 1**, where it is seen that all models provide excellent correlation with the test results. Amongst those considering shear slip deformations, the Lai-Vecchio model results in slightly better correlation in term of the ratio of computed to observed shear capacity, with a mean of 1.01 and a coefficient of variation (COV) of 10.5%. Using the MCFT, and hence ignoring crack shear slips, the accuracy is only marginally weakened with a mean of 1.03 and a COV of 10.5% for the 43 panels examined.

To gauge the accuracy of the slip models and analysis procedures for more complex structures, two series of shear walls tested by Lefas et al. (1990) were studied. The test program consisted of 13 walls tested under various conditions of axial and lateral load, wherein failure was ultimately governed by shear-compression mechanisms. The walls were of two types; either relatively squat with a height-to-width ratio of 1.0, or more slender with a height-to-width ratio of 2.0. A 340-element mesh was used to model the former, and a 536-element mesh was used for the latter; four-node (8 dof) rectangular elements were employed. The analytical results are given in **Table 2**. Excellent correlation in the calculated lateral load capacity is given by all models.

In addition to comparing calculated load capacities,

Table 1 Shear Capacities of Panel Specimens.

Beam	$v_{u\text{-}exp}$ (MPa)	$v_{u\text{-}theor}/v_{u\text{-}exp}$ 0 No slip	1 Walraven	2 Maekawa	3 Lai
PV - Series					
PV10	3.97	0.95	0.96	0.96	0.96
PV11	3.56	1.01	1.03	1.03	1.03
PV12	3.13	0.99	0.95	0.87	0.95
PV16	2.14	0.94	1.00	1.00	1.00
PV18	3.04	1.12	1.07	0.97	1.07
PV19	3.95	1.03	1.04	0.98	1.02
PV20	4.26	1.03	1.05	1.01	1.04
PV21	5.03	1.00	1.11	1.08	1.09
PV22	6.07	1.02	1.15	1.13	1.13
PV23	8.87	0.81	0.92	0.92	0.92
PV25	9.12	0.81	0.90	0.90	0.90
PV27	6.35	1.02	1.18	1.18	1.18
PV28	5.80	0.99	1.13	1.13	1.13
Mean		0.98	1.04	1.01	1.03
COV(%)		8.88	8.69	9.47	8.50
PA / PHS - Series					
PA1	6.34	0.97	0.98	0.97	0.98
PA2	6.22	0.99	0.99	0.99	0.99
PHS1	2.95	0.99	0.92	0.92	0.92
PHS2	6.66	0.97	0.90	0.77	0.90
PHS3	8.19	1.10	1.13	0.96	1.11
PHS4	6.91	1.01	0.98	0.87	0.97
PHS5	4.81	0.91	0.85	0.76	0.86
PHS6	9.89	0.88	0.94	0.91	0.90
PHS7	10.26	1.10	1.23	1.22	1.21
PHS8	10.84	0.99	1.05	1.05	1.05
PHS9	9.37	1.00	1.06	0.83	1.00
PHS10	8.58	0.99	1.03	0.93	1.02
Mean		0.99	1.01	0.93	0.99
COV(%)		6.39	10.41	13.44	9.90
PB - Series					
PB4	1.16	1.08	0.98	0.96	0.98
PB5	2.64	0.92	0.92	0.92	0.92
PB6	1.15	1.10	1.01	0.97	1.00
PB7	0.86	1.30	1.25	1.19	1.23
PB8	0.80	1.19	1.16	1.13	1.14
PB10	0.56	1.18	1.17	1.17	1.17
PB14	1.54	0.98	0.90	0.83	0.88
PB16	1.42	1.20	1.08	1.00	1.04
PB17	1.22	0.98	0.93	0.87	0.91
PB19	1.28	1.21	1.06	1.02	1.06
PB20	1.42	1.31	1.19	1.14	1.20
PB21	1.42	0.93	0.82	0.78	0.81
PB22	1.03	1.03	0.91	0.85	0.89
PB28	1.53	0.98	0.84	0.80	0.83
PB29	1.49	1.12	1.01	0.94	1.00
PB30	1.48	1.02	0.93	0.86	0.91
PB31	1.15	1.05	1.00	0.93	0.98
PB32	1.49	1.07	0.94	0.99	0.99
Mean		1.09	1.01	0.96	1.00
COV(%)		10.81	12.19	13.24	12.4
All panels					
Mean		1.03	1.02	0.97	1.01
COV(%)		10.53	10.56	12.35	10.5

Table 2 Lateral load capacities of shear wall specimens.

Wall	$v_{u\text{-}exp}$ (kN)	$v_{u\text{-}theor}/v_{u\text{-}exp}$			
		0 MCFT	1 Walraven	2 Maekawa	3 Lai
SW11	260	1.08	1.10	1.10	1.10
SW12	340	0.99	1.02	1.02	1.02
SW13	330	1.09	1.11	1.11	1.11
SW14	265	1.01	1.05	1.04	1.03
SW15	320	0.94	0.97	0.97	0.97
SW16	355	1.05	1.05	1.05	1.05
SW17	247	1.03	1.05	1.03	1.05
SW21	127	0.97	0.99	0.98	0.98
SW22	150	1.02	1.03	1.03	1.03
SW23	180	0.96	0.97	0.95	0.96
SW24	120	1.04	1.06	1.06	1.06
SW25	150	1.12	1.13	1.13	1.12
SW26	123	0.96	0.97	0.97	0.97
Mean		1.02	1.04	1.03	1.03
COV(%)		5.40	5.29	5.51	5.21

the load-deformation responses and failure modes were examined for various panel, beam and wall specimens considered. Representative results are provided by Vecchio et al. (2001). General observations are summarized below.

7. Discussion

For many of the specimens considered in the correlation studies reported above, there is not much difference in the ultimate load calculated whether slip deformations are considered (DSFM) or whether they are ignored (MCFT). [Note: The MCFT compensated for neglect of the crack slip deformations by employing a greater degree of softening in the concrete compression response.] However, there are subtle differences in predicted behaviour which are significant. Consider, for example, the calculated responses for Panel PV19 shown in **Fig. 9**. While the ultimate shear stress of the panel can be well predicted without accounting for slip deformations, the ductility in the shear stress-strain response is better simulated if crack slips are considered (see **Fig. 9(a)**). Also note that the omission of crack slips result in a slight over-prediction of the strains in the longitudinal reinforcement (**Fig. 9(b)**) and a somewhat more significant under-estimation of the strains in the transverse reinforcement (**Fig. 9(c)**) relative to the experimental values. That is, the fully-rotating crack approach, in neglecting the crack slip displacements, over-estimates the degree of stress redistribution that can occur in the element. On the other hand, the allowance for crack slips (DSFM) is seen to provide better correlation in the shear stress-strain deformation response, and in the strains in the longitudinal and transverse reinforcement. Of course, the diverging orientations of the stress and strain fields are also better represented when slip distortions are considered (see **Fig. 9(d)**), although the fully rotating model provides a reasonable estimate of the

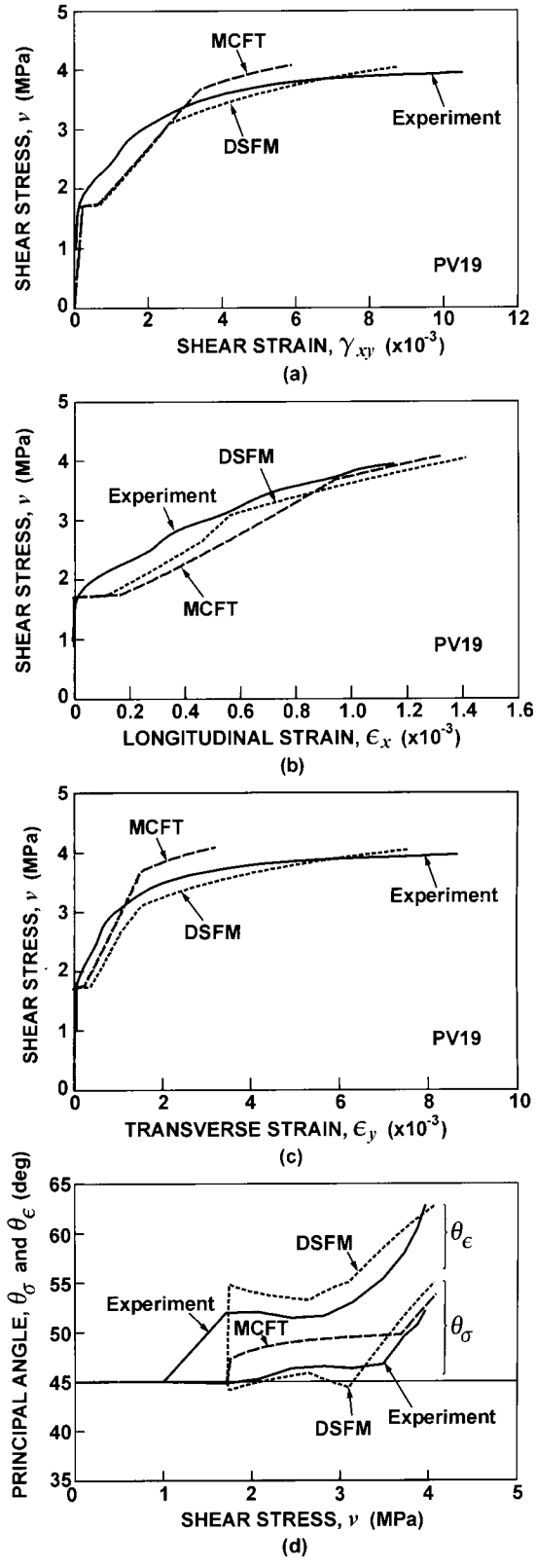

Fig. 9 Comparison of load-deformation responses for Panel PV19 (a) Shear stress-strain response (b) Longitudinal reinforcement strains (c) Transverse reinforcement strains (d) Inclination of stress and strain fields.

average value of the two. Finally, the mode of failure is better represented since, in addition to concrete strut crushing, the significant degree of sliding along the crack surfaces predicted to occur more closely corresponds to the actual observed failure mode. [In the actual test, ridging and crushing along the crack interfaces was observed.] Hence, accounting for crack shear slip results in an improved simulation of response that generally goes beyond the marginal improvement seen in predicted ultimate load capacity.

Refinements to the current model are required to further improve accuracy and reduce the significant levels of scatter seen in the data. One deficiency that exists, and should be addressed, relates to the influence of strain hardening in the reinforcement across cracks. Currently, local strain hardening effects are not considered. In reality, the local strains in the reinforcement across the cracks can be several multiples of the average strain, depending primarily on the reinforcement ratio and bond characteristics, and can reach well into strain hardening behaviour. The higher local reinforcement stresses attained through strain hardening will, in turn, influence the calculation of shear stresses on the crack surfaces, and hence the calculation of crack shear slips. Thus, a rational and consistent approach that includes local strain hardening effects will likely result in an improved calculation of crack shear slip. Allowances for a changing average crack spacing would also improve results, particularly at low and intermediate load levels. Finally, more comprehensive corroboration studies are required, with particular attention paid to effects on deformation response.

8. Conclusions

A calculation procedure was developed for calculating crack shear stresses and crack shear displacements from the average strain measurements made on reinforced concrete panels subjected to known uniform edge stresses. Several series of test panels were examined, and the crack shear stress and shear slip behaviours for these panels were determined. The experimental database thus generated was compared against the behaviour predicted by crack shear-slip relations from widely recognized models developed by other researchers. As well, an alternative constitutive relationship was proposed.

The conclusions that can be drawn from this work include the following:

1. The proposed method for determining crack shear stresses and slip displacements from panel test data appears to yield plausible results.

2. Existing crack-slip models (e.g. Walraven-Reinhardt, Okamura-Maekawa) provide reasonably good correlation to the panel test data, even though developed from data obtained from significantly different test specimens or from different analysis philosophies.

3. The alternate crack-slip constitutive model proposed produces comparable levels of accuracy to those obtained from the Walraven-Reinhardt and Okamura-Maekawa models, while providing improved facility for implementation into nonlinear finite element algorithms, improved numerical stability, and ability to consider other influencing factors.

4. Accounting for crack shear slip resulted in only slightly improved predictions of the load-deformation response and ultimate load capacity of panels and beams, relative to those obtained if crack shear slips were ignored (as in a fully rotating crack model). The calculated response of shear wall specimens showed little change.

5. However, accounting for crack shear slip was important in better capturing subtleties in response, including better estimates of reinforcement strains, post-peak ductility, and failure mode. As well, it permits consideration of the divergence in orientation of the average stress and average strain fields in the concrete, as seen in the test data.

References

Bazant, Z. P. and Gambarova, P. (1980). "Rough cracks in reinforced concrete." *J. Struct. Div., ASCE*, 106(4), 819-842.

Bhide, S. B. and Collins, M. P. (1989). "Influence of axial tension on the shear capacity of reinforced concrete members." *Amer. Concrete Inst. Struct. J.*, 86(5), 570-581.

Dei Poli, S., Gambarova, P. G. and Karakoc, C. (1987). "Aggregate interlock role in R/C thin-webbed beams in shear." *J. Struct. Engrg., ASCE*, 113(1), 1-19.

Dei Poli, S., di Prisco, M. and Gambarova, P. G. (1990). "Stress field in web of R/C thin-webbed beams failing in shear." *J. Struct. Engrg., ASCE*, 113(9), 2496-2515.

Kirschner, U. and Collins, M. P. (1986). "*Investigating the Behaviour of Reinforced Concrete Shell Elements*." Univ. of Toronto, Civil Engrg. Publication No. 86-09, pp. 82.

Lefas, I. D., Kotsovos, M. D., and Ambraseys, N. N. (1990). "Behaviour of reinforced concrete structural walls: Strength, deformation characteristics, and failure mechanism". *ACI Struct. J.*, 87(1), 23-31.

Okamura, H. and Maekawa, K. (1991). "*Nonlinear Analysis and Constitutive Models of Reinforced Concrete*." University of Tokyo, ISBN 7655-1506-0, pp. 182.

Vecchio, F. J. (2001). "Disturbed stress field model for reinforced concrete: Implementation." *J. Struct. Engrg. ASCE*, 127(1), 12-20.

Vecchio, F. J. (2000). "Disturbed stress field model for reinforced concrete: Formulation." *J. Struct. Engrg. ASCE*, 126(9), 1070-1077.

Vecchio, F. J. and Collins, M. P. (1986). "The modified compression field theory for reinforced concrete elements subjected to shear." *J. Amer. Concrete Inst.*, 83(2), 219-231.

Vecchio, F. J. and Collins, M. P. (1982). "*Response of*

Reinforced Concrete to In-Plane Shear and Normal Stresses." Report No.82-03, Dept. of Civil Engrg, Univ. of Toronto, pp. 332.

Vecchio, F. J., Collins, M. P. and Aspiotos, J. (1994). "High-strength concrete elements subjected to shear." *Amer. Conc. Inst. Struct. J.*, 91(4), 423-433.

Vecchio, F. J., Lai, D., Shim, W. and Ng, J. (2001). "Disturbed stress field model for reinforced concrete: validation." *J. Struct. Engrg. ASCE*, 127(4), 350-358.

Walraven, J. C. (1981). "Fundamental analysis of aggregate interlock." *J. Struct. Engrg, ASCE*, 107(11), 2245-2270.

Walraven, J. C. and Reinhardt, H. W. (1981). "Theory and experiments on the mechanical behaviour of cracks in plain and reinforced concrete subjected to shear loading." *Concrete Mechanics - Part A*, Heron, 26(14), pp. 65.

Appendix I: Sample calculations

Consider Panel PV19 (Vecchio and Collins, 1982) which had the following properties:

f'_c = 19.0 MPa a = 10 mm E_s = 200,000 MPa
f'_t = 1.72 MPa ρ_x = 0.01785 f_{yx} = 458 MPa
$\varepsilon_o = 2.15 \times 10^{-3}$ ρ_y = 0.00713 f_{yy} = 299 MPa

At Load Stage 7, the loading condition on the panel was:

$\sigma_x = 0$ $\sigma_y = 0$ τ_{xy} = 3.48 MPa

The average strain conditions measured were:

$\varepsilon_x = 0.716 \times 10^{-3}$ $\varepsilon_y = 1.987 \times 10^{-3}$ $\gamma_{xy} = 3.359 \times 10^{-3}$

The average crack spacing was approximately 50 mm. For this load stage, the crack shear slip and crack shear stresses are calculated as follows:

Step 1: Calculate average strains and averages stresses in the reinforcement using an elastic-plastic relationship:

$\varepsilon_{sx} = \varepsilon_x = 0.716 \times 10^{-3}$ $\varepsilon_{sy} = \varepsilon_y = 1.987 \times 10^{-3}$
$f_{sx} = E_s \cdot \varepsilon_x$ = 143.2 MPa $f_{sy} = E_s \cdot \varepsilon_{sy}$ = 299 MPa ($\leq f_{yy}$)

Step 2: Calculate average stresses in the concrete using Eqs. (11)-(13):

$f_{cx} = \sigma_x - \rho_x f_{sx} = (0.0) - (0.01785)(143.2) = -2.56$ MPa
$f_{cy} = \sigma_y - \rho_y f_{sy} = (0.0) - (0.00713)(299.0) = -2.13$ MPa
$v_{cxy} = \tau_{xy}$ = 3.48 MPa

Step 3: Using standard stress transformations, determine average principal stresses in the concrete:

$$f_{c1}, f_{c2} = \frac{(f_{cx} + f_{cy})}{2} \pm \frac{1}{2}[(f_{cx} - f_{cy})^2 + 4 v_{cxy}^2]^{1/2}$$
$$= 1.14, -5.83 \text{ MPa}$$

$$\theta_\sigma = \frac{\pi}{2} - \frac{1}{2}\tan^{-1}\left[\frac{2 v_{cxy}}{f_{cy} - f_{cx}}\right] = 46.8°$$

Step 4: Find local stresses in the reinforcement by using Eqs. (14)-(15) and satisfying equilibrium conditions Eq. (16).

$\varepsilon_{scrx} = 0.716 \times 10^{-3} + \Delta\varepsilon_{1cr} \cdot \cos^2 46.8°$
$\varepsilon_{scry} = 1.987 \times 10^{-3} + \Delta\varepsilon_{1cr} \cdot \sin^2 46.8°$
$f_{scrx} = E_s \cdot \varepsilon_{scrx} \leq f_{yx}$
$f_{scry} = E_s \cdot \varepsilon_{scry} \leq f_{yy}$

$(0.01785)(f_{scrx} - 143.2)\cos^2 46.8° + (0.00713)(f_{scry} - 299)\sin^2 46.8° = 1.14$ (MPa)
$\rightarrow \Delta\varepsilon_{1cr} = 1.454 \times 10^{-3}$
f_{scrx} = 279.5 MPa f_{scry} = 299.0 MPa

Step 5: Using Eq. (17), calculate shear stresses on the crack surface:

$v_{ci} = (0.01785)(279.5 - 143.2)\cos 46.8° \sin 46.8° - (0.00713)(299 - 299)\sin 46.8° \cos 46.8°$
$= 1.21$ MPa

Step 6: Using Eq. (10), calculate average shear slip strain:

$\gamma_s = \gamma_{xy}\cos 2\theta_a + (\varepsilon_y - \varepsilon_x)\sin 2\theta_a$
$= (3.359 \times 10^{-3})\cos 93.6° + (1.987 \times 10^{-3} - 0.716 \times 10^{-3})\sin 93.6°$
$= 1.058 \times 10^{-3}$

Step 7: From Eq. (9), determine shear slip along the crack surface:

$\delta_s = \gamma_s \cdot s = (1.058 \times 10^{-3})(50.0) = 0.053$ mm

Notation

- a = aggregate size (mm);
- E_c = initial modulus of elasticity of concrete;
- E_s = elastic modulus of reinforcing steel;
- f'_c = compressive strength of concrete cylinder (28 days);
- f'_t = tensile strength of concrete;
- f_{cc} = compressive strength of concrete cube;
- f_{c1} = principal tensile stress in concrete (in 1-direction);
- f_{c2} = principal compressive stress in concrete (in 2-direction);
- f_s = average stress in reinforcement;
- f_{scr} = local stress (at crack) in reinforcement;
- f_y = yield stress of reinforcement;
- s = average crack spacing in 1-direction;
- v_c = shear stress on concrete relative to reference x,y-directions;
- v_{ci} = shear stress on crack surface;
- v_{cmax} = maximum shear stress that can be resisted on crack surface;
- w = average crack width;
- γ_s = shear strain due to slip along crack surface;
- $\Delta\varepsilon_{1cr}$ = local incremental strain in 1-direction at crack locations;
- δ_s = slip displacement along crack surface;
- δ^e_s = experimental slip displacement (from test panel);
- δ^t_s = theoretical slip displacement (from constitutive model);

$[\varepsilon]$ = apparent (total) average strains in element, including crack slip strains;
$[\varepsilon_c]$ = average strains in concrete, net of crack slip strains;
ε_{c1} = strain in concrete in principal tensile stress direction;
ε_{c2} = strain in concrete in principal compressive stress direction;
ε_s = average strain in reinforcement;
ε_o = compression strain at peak stress f'_c in concrete cylinder (negative value);
θ = inclination of normal to crack direction in concrete;
θ_ε = inclination of apparent (total) principal strains in concrete;
θ_σ = inclination of principal stresses in concrete;
ρ = reinforcement ratio; and
$[\sigma]$ = average stresses acting on element.